PHYSICAL REVIEW C

NUCLEAR PHYSICS

THIRD SERIES, VOLUME 58, NUMBER 5 NOVEMBER 1998

RAPID COMMUNICATIONS

The Rapid Communications section is intended for the accelerated publication of important new results. Manuscripts submitted to this section are given priority in handling in the editorial office and in production. A Rapid Communication in **Physical Review C** *may be no longer than five printed pages and must be accompanied by an abstract. Page proofs are sent to authors.*

High-spin states in the odd-odd $N=Z$ nucleus ^{50}Mn

C. E. Svensson,[1] S. M. Lenzi,[2] D. R. Napoli,[3] A. Poves,[4] C. A. Ur,[2,5] D. Bazzacco,[2] F. Brandolini,[2] J. A. Cameron,[1] G. de Angelis,[3] A. Gadea,[3] D. S. Haslip,[1] S. Lunardi,[2] E. E. Maqueda,[6] G. Martínez-Pinedo,[7] M. A. Nagarajan,[8] C. Rossi Alvarez,[2] A. Vitturi,[2] and J. C. Waddington[1]

[1]*Department of Physics and Astronomy, McMaster University, Hamilton, Ontario, Canada L8S 4M1*

[2]*Dipartimento di Fisica and INFN, Sezione di Padova, Padova, Italy*

[3]*Laboratori Nazionali di Legnaro, INFN, Legnaro, Italy*

[4]*Departamento de Física Teórica C-XI, Universidad Autónoma de Madrid, E-28049 Madrid, Spain*

[5]*H. Hulubei National Institute of Physics and Nuclear Engineering, Bucharest, Romania*

[6]*Departamento de Física, CNEA, and CONICET, Argentina*

[7]*University of Aarhus, Aarhus, Denmark*

[8]*Department of Physics, UMIST, Manchester, United Kingdom*

(Received 20 July 1998)

High-spin states in the odd-odd $N=Z$ nucleus ^{50}Mn have been identified. At low spin, the $T=1$ isobaric analogue states of ^{50}Cr are established up to $I^{\pi}=4^{+}$. At high spin, the $T=0$ band built on the low-lying $I^{\pi}=5^{+}$ isomer in ^{50}Mn becomes energetically favored and this band is observed up to its $f_{7/2}$-shell termination at $I^{\pi}=15^{+}$. Spherical shell model calculations in the full pf shell are found to be in excellent agreement with the experimental results. In addition, a weak side band in ^{50}Mn is observed to spin (12^{-}) and is interpreted as a possible octupole vibrational structure. [S0556-2813(98)50211-7]

PACS number(s): 23.20.Lv, 27.40.+z, 21.60.Cs, 21.10.Hw

Recent advances in both experimental and theoretical techniques have enabled detailed studies of high-spin states in many of the $N\approx Z$ nuclei in the $1f_{7/2}$ shell. Near the middle of this shell, the number of valence particles/holes (8 in ^{48}Cr) is large enough to lead to collective behavior [1–4], yet small enough that the maximum spin available in pure $f_{7/2}$-shell configurations is limited to experimentally observable values and noncollective band-terminating states have recently been identified in several of these nuclei [2–5]. As one moves away from the middle of the $f_{7/2}$ shell, the doubly-magic spherical nuclei ^{40}Ca and ^{56}Ni are rapidly approached. The collective behavior observed near the middle of the shell thus gives way to more pronounced shell model effects [6]. The $f_{7/2}$-shell nuclei thus provide an excellent opportunity to study the interplay between collective and single-particle degrees of freedom as functions of both angular momentum and valence particle number. Recent studies of high-spin states in these nuclei have also shed new light on the cross-conjugate symmetry resulting from simultaneous proton-neutron and particle-hole exchange in the $f_{7/2}$ shell [5], as well as the more generally applicable mirror symmetry resulting from proton-neutron exchange [7–10].

Parallel progress has been made in the theoretical study of $f_{7/2}$-shell nuclei. Recent advances in large-scale shell model calculations have enabled computations for these nuclei involving the full pf shell model space [11,12]. Of particular interest have been theoretical studies of ^{48}Cr [13] and ^{50}Cr [14] in which large-scale shell model calculations have been compared with the results of cranked Hartree-Fock-Bogoliubov calculations. The collective nuclei in the middle of the $f_{7/2}$ shell have thus provided the opportunity for new insights into the relationship between the microscopic shell model description of nuclei in the laboratory frame and the mean-field cranking description of the nuclear intrinsic state.

Despite the many recent advances in the study of $N\approx Z$ $f_{7/2}$-shell nuclei, there remains a notable deficiency of high-spin data for the odd-odd $N=Z$ nuclei in this region. In particular, the spectroscopic data for ^{50}Mn have not been

extended since King *et al.* [15] identified γ-ray transitions between low-lying states with the light-ion reaction ^{50}Cr$(p,n\gamma)^{50}$Mn more than 25 years ago. Odd-odd $N=Z$ nuclei are, however, of particular interest because they offer the best opportunity to investigate the interplay between isospin $T=0$ and $T=1$ neutron-proton pairing [16–20] as a function of angular momentum. The odd-odd $N=Z$ nuclei in the $f_{7/2}$ shell have $T=1$, $I^{\pi}=0^{+}$ ground states. However, $T=0$ bands are expected to be favored at high spin. In this work we report the first observation of high-spin states in ^{50}Mn. The $T=1$ isobaric analogue states of ^{50}Cr are established up to spin 4^{+}, and the energetically favored $T=0$ band built on the low-lying 5^{+} isomer in ^{50}Mn is observed up to its $f_{7/2}$-shell termination at $I^{\pi}=15^{+}$. A weak side band is also observed in ^{50}Mn and is interpreted as a possible octupole vibrational structure.

High-spin states in ^{50}Mn were populated via the ^{28}Si$(^{28}$Si$,\alpha pn)^{50}$Mn reaction, with a 115-MeV ^{28}Si beam provided by the XTU Tandem Accelerator at the Legnaro National Laboratory. The target consisted of 0.8 mg/cm^2 of ^{28}Si evaporated on a 13 mg/cm^2 Au backing. Gamma rays were detected with the GASP array [21], comprising 40 Compton-suppressed HPGe detectors and an 80-element bismuth germanate (BGO) ball which acts as a γ-ray multiplicity and sum-energy filter. Charged particles were detected with the ISIS array [22], a 4π detector consisting of 40 $(\Delta E,E)$ Si telescopes. During the experiment, 8.4×10^{8} events were recorded in which at least two HPGe detectors and at least two elements of the BGO ball fired in coincidence.

Based on measured γ-ray intensities, the αpn evaporation channel leading to ^{50}Mn was estimated to represent only $\sim$1% of the total fusion cross section in this experiment. In order to analyze this weak channel, a γ-γ coincidence matrix was constructed for all events in which one proton and one alpha particle were detected in the ISIS array. Contamination in this matrix due to events from the much stronger ^{50}Cr$(\alpha 2p)$, ^{49}Cr$(\alpha 2pn)$, ^{49}V$(\alpha 3p)$, and ^{47}V$(2\alpha p)$ channels was largely removed by subtracting properly normalized fractions of the $\alpha 2p$, $\alpha 3p$, and $2\alpha p$ gated γ-γ matrices. This subtracted matrix was found to provide the best combination of clean channel selection and statistical quality for constructing the decay scheme of ^{50}Mn. The coincidence relationships deduced from this matrix were also confirmed by double gating on the ^{50}Mn γ rays in a γ-γ-γ coincidence cube.

The decay scheme for ^{50}Mn deduced from the present work is shown in Fig. 1, and γ-ray spectra obtained by setting coincidence gates in the ''clean'' ^{50}Mn matrix are shown in Fig. 2. The spin assignments shown in Fig. 1 were deduced from the γ-ray angular distributions and from directional correlation from oriented state (DCO) ratios. The 0^{+}, 2^{+}, and 4^{+} states in ^{50}Mn at excitation energies of 0, 800, and 1917 keV are interpreted as the $T=1$ isobaric analogues of the 0, 783, and 1882 keV states in ^{50}Cr [4,5]. We note that these $T=1$ states, and the 1^{+} and 3^{+} $T=0$ states connected to them by $M1$ transitions, were populated very weakly in this experiment ($\sim$2% of the ^{50}Mn channel intensity) and it was not possible to extend the $T=1$ band to higher spin. This weak population of the ground band results from the highly non-yrast nature of this band at high spin where the

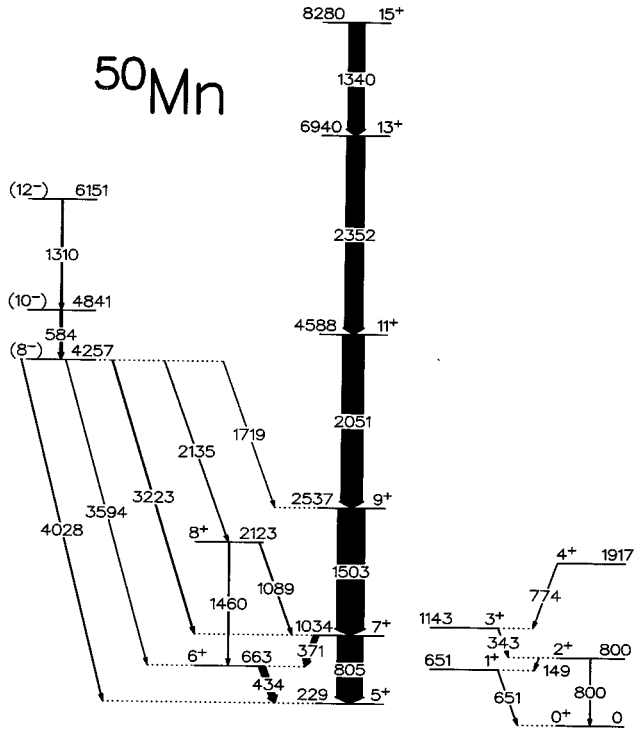

FIG. 1. Level scheme of ^{50}Mn from the present work. Transition and level energies are given to the nearest keV. The excitation energy of the 5^{+} isomer is taken from Ref. [23].

$T=0$ band built on the low-lying 5^{+} isomer in ^{50}Mn becomes strongly favored. As indicated in Fig. 1, the majority of the ^{50}Mn channel intensity is collected by this $T=0$ band and decays to the 5^{+} isomer (which β^{+} decays to ^{50}Cr with a halflife of 1.75 min [23]). We were unable to identify any transitions linking this $T=0$ band to the low-spin $T=0$ and $T=1$ states which feed the 0^{+} ground state. The excitation energy of the 5^{+} isomer was therefore not established by this work. The value of 229 keV indicated in Fig. 1 has been taken from the literature and has an uncertainty of ±7 keV [23]. The 805 keV transition between the 7^{+} and 5^{+} $T=0$ states in ^{50}Mn was tentatively assigned previously [15]. We have confirmed this assignment, and extended the $T=0$ band to $I^{\pi}=15^{+}$, the maximum spin available to ^{50}Mn in a pure $f_{7/2}$-shell configuration. In addition, a weak side band was observed in ^{50}Mn up to $I^{\pi}=(12^{-})$ and, as shown in Fig. 2(b), five high-energy transitions linking the 4257 keV state of this structure to the 5^{+}, 6^{+}, 7^{+}, 8^{+}, and 9^{+} $T=0$ states were identified. Although the limited statistics for these high-energy transitions prevented a definite spin/parity assignment for the 4257 keV state, the angular distribution measurements favor our tentative (8^{-}) assignment. As discussed below, an octupole vibration coupled to the 5^{+} $T=0$ state provides a possible explanation for the observed decay pattern of this structure.

As noted above, excellent agreement has recently been demonstrated between experimental data and full pf shell model calculations for a number of nuclei in this mass region [11–14]. In order to test further the accuracy of these large-scale shell model calculations and to obtain a more complete understanding of the new experimental results, we have performed full pf shell model calculations for ^{50}Mn. The KB3

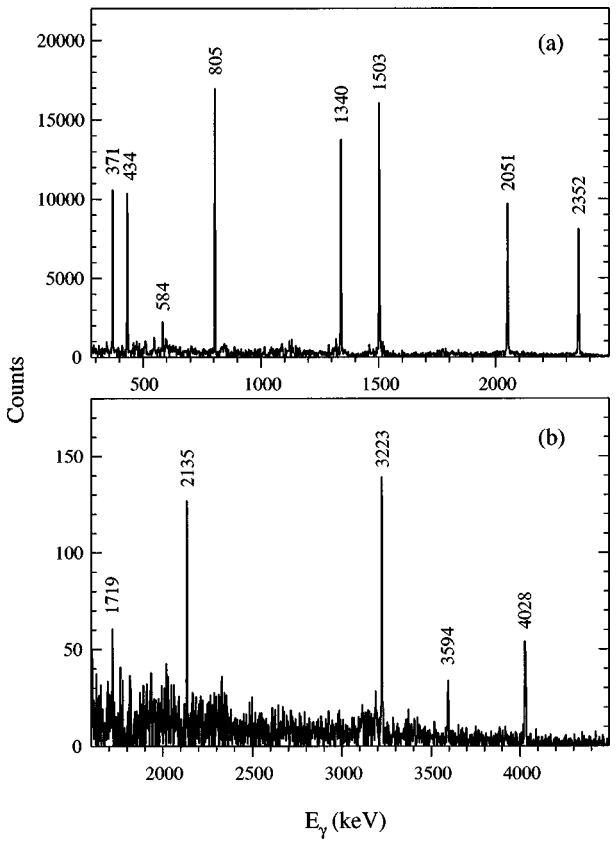

FIG. 2. γ-ray spectra generated by setting coincidence gates in the ''clean'' ^{50}Mn γ-γ matrix (see text for details). (a) Sum of gates on the strong transitions in the $T=0$ band. (b) The high-energy portion of the γ-ray spectrum in coincidence with the 584 keV transition showing the five transitions linking the 4257 keV (8^-) state to the low-lying $T=0$ states.

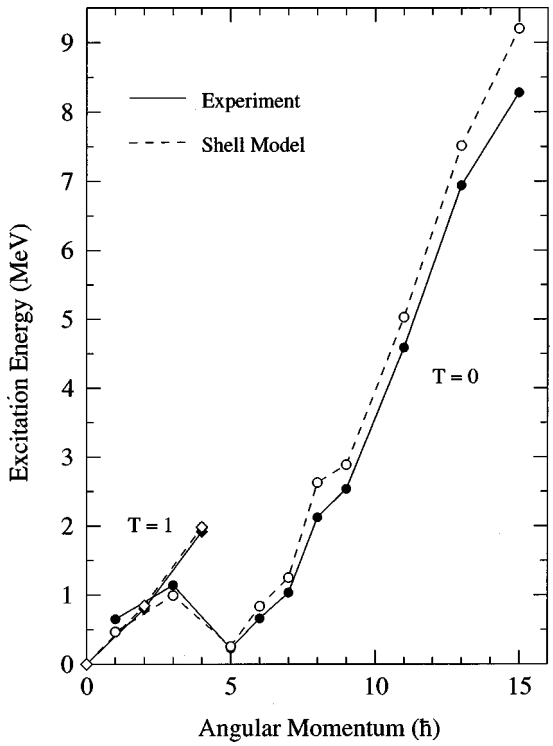

FIG. 3. Excitation energy versus angular momentum for states in ^{50}Mn. The experimental data (solid lines and filled symbols) are compared with full pf shell model calculations (dashed lines and open symbols). $T=0$ and $T=1$ states are indicated by circles and diamonds, respectively.

interaction [24] was used and the single-particle energies were taken from the experimental spectrum of ^{41}Ca. The Hamiltonian was diagonalized with the code ANTOINE [25]. The theoretical spectrum for ^{50}Mn obtained from these calculations is compared with the experimental data in Fig. 3. Although the experimental spectrum is slightly more compressed than its shell model counterpart, the overall agreement between theory and experiment is excellent.

A more sensitive test of the shell model calculations is obtained from a comparison of the calculated transition matrix elements with experimental values deduced from lifetime measurements. Unfortunately, accurate lifetime measurements for the states in ^{50}Mn were not possible in this experiment because of the long lifetime of the 15^+ terminating state. No Doppler-broadened peak shape was observed for the 1340 keV transition, indicating that the terminating state decayed after the ^{50}Mn recoils were fully stopped in the target backing. While this led to sharp γ-ray peaks for all of the transitions in the $T=0$ band (see Fig. 2) and facilitated the observation of this structure, it precluded the possibility of measuring lifetimes for the lower-spin states because all of the peak shapes simply reflected the long lifetime of the terminating state. Small Doppler-broadened components resulting from fast side feeding were observed for the 2352, 2051, and 1503 keV transitions. However, the large uncertainties in the ratios of this weak side feeding to the strong top feeding of these states, combined with the usual uncertainties in the time structure of the unobserved side feeding, prevented a meaningful quantitative analysis of the state lifetimes. It should, however, be noted that the fully stopped peak shape for the 1340 keV transition implies a lifetime larger than the recoil stopping time ($\sim$2 ps), while the broadened components for the 2352, 2051, and 1503 keV transitions can only result from the combination of fast side feeding and state lifetimes shorter than the stopping time. These observations are, at least qualitatively, in agreement with the lifetimes of 4.0, 0.11, 0.17, and 0.80 ps for the 15^+, 13^+, 11^+, and 9^+ states calculated from the shell model $B(E2)$ values shown in Table I and the experimental transition energies. The terminating 15^+ state in ^{50}Mn is obtained by fully aligning the valence particles in the $(f_{7/2})^{10}$ configuration and the long lifetime of this state results from its noncollective nature. This transition to a noncollective state is indicated by the sudden decrease in the calculated $B(E2)$ values as the terminating state is reached.

Although absolute state lifetimes could not be accurately measured in this experiment, quantitative tests of a number of the shell model transition matrix elements could be made based on measured branching ratios. Table II compares branching ratios calculated with the theoretical $B(E2)$ and $B(M1)$ values (and the experimental transition energies) with the observed values. The agreement between theory and experiment is, in general, very good. The very large calculated $M1(\Delta T=1)/E2(\Delta T=0)$ branching ratios among the low-spin states also provide a natural explanation for the failure to observe the $3^+\rightarrow 1^+$ and $4^+\rightarrow 2^+$ $E2$ transitions

TABLE I. Reduced matrix elements for transitions in ^{50}Mn from the shell model calculations.

I_i^π	I_f^π	$B(E2)$ (e^2 fm^4)	$B(M1)$ (μ_N^2)
$1^+_{T=0}$	$0^+_{T=1}$		2.16
$2^+_{T=1}$	$1^+_{T=0}$		2.09
$3^+_{T=0}$	$2^+_{T=1}$		2.57
$4^+_{T=1}$	$3^+_{T=0}$		2.95
$2^+_{T=1}$	$0^+_{T=0}$	189	
$4^+_{T=1}$	$2^+_{T=0}$	208	
$3^+_{T=0}$	$1^+_{T=0}$	240	
$6^+_{T=0}$	$5^+_{T=0}$	258	
$7^+_{T=0}$	$6^+_{T=0}$	251	
$7^+_{T=0}$	$5^+_{T=0}$	42	
$8^+_{T=0}$	$7^+_{T=0}$	140	
$8^+_{T=0}$	$6^+_{T=0}$	74	
$9^+_{T=0}$	$8^+_{T=0}$	142	
$9^+_{T=0}$	$7^+_{T=0}$	133	
$11^+_{T=0}$	$9^+_{T=0}$	130	
$13^+_{T=0}$	$11^+_{T=0}$	99	
$15^+_{T=0}$	$13^+_{T=0}$	47	

in this experiment. We note that the $8^+ \rightarrow 7^+$, $7^+ \rightarrow 6^+$, and $6^+ \rightarrow 5^+$ transitions are of electric quadrupole character due to the hindrance of magnetic dipole transitions between $T=0$ states in self-conjugate nuclei [26].

In a recent paper, Martínez-Pinedo *et al.* [12] studied the $A=47$ and 49 nuclei in the framework of the full pf spherical shell model. In the case of the mirrors ^{49}Cr and ^{49}Mn, a strong-coupling limit particle-plus-rotor scheme was shown to fit the ground state bands up to the backbending at $17/2^-$. The rotor behavior was further supported by the rather constant intrinsic quadrupole moments obtained from the calculated $B(E2)$'s (Q_0^t) *and* from the static quadrupole moments $Q_s(Q_0^s)$, although a change of regime was noticed at $I=13/2$ before the backbending. In Table III we show the corresponding values for the $T=0$ band of ^{50}Mn, in which a nucleon is added to the odd-A mirrors. The two-particle-plus-rotor strong-coupling limit implies constant Q_0 values up to $I \sim 10$ in ^{50}Mn. As can be seen in Table III, both

TABLE II. Branching ratios (B) for transitions in ^{50}Mn from the present experiment and shell model calculations.

I_i^π	I_f^π	B_{exp}(%)	B_{theo}(%)
2^+	1^+	62 (18) ($M1$)	61 ($M1$)
	0^+	38 (18) ($E2$)	39 ($E2$)
3^+	2^+	100 (25) ($M1$)	99 ($M1$)
	1^+		1 ($E2$)
4^+	3^+	100 (25) ($M1$)	98 ($M1$)
	2^+		2 ($E2$)
7^+	6^+	15 (1.7) ($E2$)	11 ($E2$)
	5^+	85 (1.7) ($E2$)	89 ($E2$)
8^+	7^+	47 (16) ($E2$)	69 ($E2$)
	6^+	53 (16) ($E2$)	31 ($E2$)
9^+	8^+		1 ($E2$)
	7^+	100 (3.7) ($E2$)	99 ($E2$)

TABLE III. Shell model static quadrupole moments Q_s, the corresponding intrinsic quadrupole moments Q_0^s, and the intrinsic quadrupole moments Q_0^t deduced from the $B(E2)$ values.

			Q_0^t (e fm^2)	
I^π	Q_s (e fm^2)	Q_0^s (e fm^2)	$\Delta I=1$	$\Delta I=2$
5^+	57	98		
6^+	32	102	93	
7^+	14	100	84	92
8^+	5	285	64	87
9^+	-0.6	9	68	97
11^+	0.5	-2.6		80
13^+	6	-23		64
15^+	25	-80		41

calculated intrinsic quadrupole moments Q_0^s and Q_0^t are similar and rather constant at low spin, but a change of regime appears at $I=8$ where the calculated Q_0 values start to behave erratically. In fact, the 10^+ state, which was not observed in this experiment, is calculated to lie above the 11^+ state.

Unnatural-parity side bands have been identified in several nuclei in this mass region (e.g., ^{45}Sc, ^{45,46}Ti, ^{47}V, ^{48,49,50}Cr) and have been explained in terms of pf-shell configurations with a hole excitation in the $d_{3/2}$ orbital [27–29]. However, this is not the case for ^{52}Fe, in which an octupole vibration provides a better explanation of the observed 3^- bandhead at 4396 keV [6]. Similarly, the (proposed) negative parity structure in ^{50}Mn starting at the 4257 keV, $I^\pi=(8^-)$ state could be explained as an octupole vibration coupled to the 5^+ $T=0$ state. This interpretation would provide a natural explanation for the successful competition of $E3$ decay with $E1$ decay of the (8^-) state. Unfortunately, a shell model description of such structures, which should involve contributions from both hole excitations in the sd shell and particle excitations to the $g_{9/2}$ orbital, in addition to the full pf shell, is beyond present computational capabilities.

As noted above, odd-odd $N=Z$ nuclei offer the opportunity to investigate the interplay between $T=0$ and $T=1$ pairing interactions. In particular, both pairing modes in the proton-neutron channel play a dominant role in these nuclei, while their contribution decreases rapidly with a moderate neutron or proton excess. It was also noted above that in the $f_{7/2}$ shell, all odd-odd self-conjugate nuclei have $I^\pi=0^+$, $T=1$ ground states. This differs from lighter odd-odd $N=Z$ nuclei, in which $I \neq 0$, $T=0$ ground states are favored. In a recent paper [30], a possible explanation for this behavior was suggested in the framework of the spherical shell model with the KB3 interaction. It was argued that the inversion of $T=0$ and $T=1$ configurations arises from the balance between the isovector monopole term, which has a smooth dependence on mass, and isoscalar and isovector pairing interactions. This latter term depends linearly on the degeneracy of the valence orbit. Therefore, when a high-j orbit comes into play, the $T=1$ state should become the ground state. The strong influence of the isovector proton-neutron correlations on the properties of ^{50}Mn at low temperature has also been pointed out in Ref. [16] within shell model Monte Carlo calculations.

It is also interesting to note that, while the proton-neutron $(f_{7/2})^2$ $T=0$ interaction favors the $I=1$ and $I=7$ couplings (cf. ^{42}Sc), the strong quadrupole field near the middle of the shell gives rise to a 5^+ bandhead in ^{50}Mn, corresponding to a proton-neutron pair in the [312]5/2 Nilsson orbit.

In summary, high-spin states have been identified in the odd-odd $N=Z$ nucleus ^{50}Mn. The $T=1$ isobaric analogue states of ^{50}Cr have been established to $I^\pi=4^+$, while at high-spin the energetically favored $T=0$ band has been observed up to its $f_{7/2}$-shell band termination at $I^\pi=15^+$. Excellent agreement is found between the experimental results and spherical shell model calculations in the full pf shell. A weak side band of proposed negative parity has also been identified in ^{50}Mn and the decay pattern of the (8^-) bandhead of this structure suggests an interpretation based on an octupole vibration coupled to the low-lying 5^+ $T=0$ isomeric state.

We are grateful to B. F. Bayman and A. P. Zuker for fruitful discussions. C.E.S., J.A.C., D.S.H., and J.C.W. were supported by the Natural Science and Engineering Research Council of Canada, A.G. was supported by the EC under contract ERBCHBGCT940713, and A.P. was supported by DGES (Spain) under grant PB96-053. G. Manente is acknowledged for the skillful target preparation.

[1] J. A. Cameron, M. A. Bentley, A. M. Bruce, R. A. Cunningham, W. Gelletly, H. G. Price, J. Simpson, D. D. Warner, and A. N. James, Phys. Rev. C **49**, 1347 (1994).
[2] J. A. Cameron *et al.*, Phys. Lett. B **387**, 266 (1996).
[3] S. M. Lenzi *et al.*, Z. Phys. A **354**, 117 (1996).
[4] S. M. Lenzi *et al.*, Phys. Rev. C **56**, 1313 (1997).
[5] J. A. Cameron *et al.*, Phys. Rev. C **58**, 808 (1998).
[6] C. A. Ur *et al.*, Phys. Rev. C (to be published).
[7] J. A. Cameron, M. A. Bentley, A. M. Bruce, R. A. Cunningham, W. Gelletly, H. G. Price, J. Simpson, D. D. Warner, and A. N. James, Phys. Lett. B **235**, 239 (1990).
[8] J. A. Cameron, M. A. Bentley, A. M. Bruce, R. A. Cunningham, H. G. Price, J. Simpson, D. D. Warner, A. N. James, W. Gelletly, and P. Van Isacker, Phys. Lett. B **319**, 58 (1993).
[9] C. D. O'Leary, M. A. Bentley, D. E. Appelbe, D. M. Cullen, S. Ertürk, R. A. Bark, A. Maj, and T. Saitoh, Phys. Rev. Lett. **79**, 4349 (1997).
[10] D. Rudolph *et al.*, Z. Phys. A **358**, 379 (1997).
[11] E. Caurier, A. P. Zuker, A. Poves, and G. Martínez-Pinedo, Phys. Rev. C **50**, 225 (1994).
[12] G. Martínez-Pinedo, A. P. Zuker, A. Poves, and E. Caurier, Phys. Rev. C **55**, 187 (1997).
[13] E. Caurier, J. L. Egido, G. Martínez-Pinedo, A. Poves, J. Retamosa, L. M. Robledo, and A. P. Zuker, Phys. Rev. Lett. **75**, 2466 (1995).
[14] G. Martínez-Pinedo, A. Poves, L. M. Robledo, E. Caurier, F. Nowacki, J. Retamosa, and A. Zuker, Phys. Rev. C **54**, R2150 (1996).
[15] N. S. P. King, C. E. Moss, H. W. Baer, and R. A. Ristinen, Nucl. Phys. **A177**, 625 (1971).
[16] K. Langanke, D. J. Dean, S. E. Koonin, and P. B. Radha, Nucl. Phys. **A613**, 253 (1997).
[17] D. Rudolph *et al.*, Phys. Rev. Lett. **76**, 376 (1996).
[18] S. Frauendorf, J. A. Sheikh, and N. Rowley, Phys. Rev. C **50**, 196 (1994).
[19] J. A. Sheikh, N. Rowley, M. A. Nagarajan, and H. G. Price, Phys. Rev. Lett. **64**, 376 (1990).
[20] J. A. Sheikh, N. Rowley, and M. A. Nagarajan, Phys. Lett. B **240**, 11 (1990).
[21] D. Bazzacco, in Proceedings of the International Conference on Nuclear Structure at High Angular Momentum, edited by J. C. Waddington and D. Ward, Report No. AECL 10613, Vol. 2, p. 376, 1992.
[22] E. Farnea, *et al.*, in Laboratori Nazionali di Legnaro Annual Report 1994, edited by A. M. Stefanini, E. Fioretto, and D. R. Napoli, Report No. LNL-INFN-095/95, p. 189, 1995.
[23] T. W. Burrows, Nucl. Data Sheets **75**, 88 (1995).
[24] A. Poves and A. Zuker, Phys. Rep. **70**, 235 (1981).
[25] E. Caurier, code ANTOINE, Strasbourg, 1989, unpublished.
[26] E. K. Warburton and J. Weneser, in *Isospin in Nuclear Physics*, edited by D. H. Wilkinson (North-Holland, Amsterdam, 1969), Chap. 5.
[27] P. Bednarczyk *et al.*, Eur. Phys. J. A **2**, 157 (1998).
[28] A. Poves and J. Sánchez-Solano, Phys. Rev. C **58**, 172 (1998).
[29] F. Brandolini *et al.*, Nucl. Phys A (in press).
[30] A. Poves and G. Martínez-Pinedo, Phys. Lett. B **430**, 203 (1998).